LA-UR- 10-03245

Approved for public release; distribution is unlimited.

Title: Modeling gated neutron images of THD capsules

Author(s): D. Wilson, G. Grim, I. Tregillis, M. Wilke, M. Patel, S. Sepke, G. Morgan, R. Hatarik, E. Loomis, C. Wilde, J. Oertel, V. Fatherley, D. Clark, D. Fittinghoff, D. Bower, M. Schmitt, M. Marinak, D. Munro, F. Merrill, M. Moran, T.-S. Wang, C. Danly, R. Hilko, S. Batha, M. Frank, R. Buckles

Intended for: High Temperature Plasma Diagnostics Conference 2010 Wildewood, NJ, May 16-20 2010 and for Reviews of Scientific Instruments

Los Alamos
NATIONAL LABORATORY
EST. 1943

Modeling gated neutron images of THD capsules

D. Wilson[1], G. Grim[1], I. Tregillis[1], M. Wilke[1], M. Patel[2], S. Sepke[2], G. Morgan[1], R. Hatarik[2], E. Loomis[1], C. Wilde[1], J. Oertel[1], V. Fatherley[1], D. Clark[1], D. Fittinghoff[2], D. Bower[2], M. Schmitt[1], M. Marinak[2], D. Munro[2], F. Merrill[1], M. Moran[2],T.-S. Wang[1], C. Danly[1], R. Hilko[3], S. Batha[1], M. Frank[2], R. Buckles[3]

[1]Los Alamos National Laboratory, Los Alamos, New Mexico, 87545

[2]Lawrence Livermore National Laboratory, Livermore, CA. 94551

[3]NSTEC, Los Alamos, NM 87544

Abstract

Time gating a neutron detector 28m from a NIF implosion can produce images at different energies. The brighter image near 14 MeV reflects the size and symmetry of the capsule "hot spot". Scattered neutrons , ~9.5-13 MeV, reflect the size and symmetry of colder, denser fuel, but with only ~1-7% of the neutrons. The gated detector records both the scattered neutron image, and, to a good approximation, an attenuated copy of the primary image left by scintillator decay. By modeling the imaging system the energy band for the scattered neutron image (10-12 MeV) can be chosen, trading off the decayed primary image and the decrease of scattered image brightness with energy. Modeling light decay from EJ399, BC422, BCF99-55, Xylene, DPAC-30, and Liquid A leads to a preference from BCF99-55 for the first NIF detector, but DPAC 30 and Liquid A would be preferred if incorporated into a system. Measurement of the delayed light from the NIF scintillator using implosions at the Omega laser shows BCF99-55 to be a good choice for down-scattered imaging at 28m.

Corresponding author address: MS B269, Los Alamos National Laboratory, Los Alamos, NM 87545.

Contributed paper, published as part of the Proceedings of the 18th Topical Conference on High-Temperature Plasma Diagnostics, Wildewood, New Jersey, May 2010.

I. INTRODUCTION

Imaging thermonuclear neutrons from the D+T reaction as been used to diagnose ICF capsule performance[1,2,3] and will be used at the National Ignition Facility (NIF)[4] . Since the imploded capsules at the Omega laser[5] and NIF are relatively thin to neutrons, images of neutrons escaping near the Doppler broadened 14 MeV peak show where they were generated, a small (~ 25 μm radius), hot (~3-10 keV) spot. However at DT areal densities of 1-2 g/cm^2 expected at NIF, 20-40% of DT neutrons experience one or occasionally more collisions in the capsule. Imaging those scattered neutrons has been proposed[6,7,8] to diagnose the location of all the fuel in a capsule, both hot and cold. Due to low fuel areal densities no down-scattered images have yet been obtained. Because T+T reactions produce a continuum of neutrons between 0 and 9.5 MeV, generated in the hot spot, the 10-12 MeV band has been chosen for most analysis.

We have modeled the NIF neutron imaging system[9] performance needed to obtain both primary and down-scattered images, evaluated several potential scintillators, and measured the performance of the first NIF imaging scintillator on the Omega laser.

II. Modeling the NIF Neutron Imaging System (NIS)

The model begins with 2D hydrodynamic calculations of an ICF capsule. The implosion of a germanium doped plastic[10] THD[11] capsule is calculated in using the HYDRA code[12] using Monte Carlo neutron and charged particle transport. Escaping neutrons are tabulated and analyzed in 50keV wide energy bins between 0 and 20 MeV. Their locations and directions are used to form 100x100 images with 2x2 μm pixels. This 400x100x100 array is the neutron source for our simulations.

The NIS aperture is a set of 37 sub-apertures ("pinholes") in a 20 cm long tungsten block located 26.5 cm from the target[13]. The field of view of each sub-aperture is a square with an inscribed circle of either 140 or 210 μm in the source plane. The point spread function for one sub-aperture depends upon the source location. To represent this, each point in a 250x250 source plane has its own 250x250 point spread function[14]. The neutron source can be located off the centerline of the pinhole aperture. In a forward model the placed source is convolved with the 250^4 element psf. When analyzing the experimental data, the position and brightness of sub-aperture images at the detector allow us to determine the source position w.r.t. the aperture axis. This position is then used in the deconvolution of the aperture psf to obtain our best estimate of the source[15].

III. Modeling Scintillator Decay and the Down-Scattered Image

Neutron energy discrimination is obtained by gating the scintillator light on and off at the neutron energy arrival times. The energy bins become arrival time bins. This is modeled as a 400x100x100 array of excited state populations in the scintillator. Light is produced from this excited state with characteristic scintillator decay times. The location of the NIF scintillator at 28 m from the capsule determines the arrival time of 10 and 12 MeV neutrons after the 14 MeV peak. To study the utility of various scintillators we modeled light collected in down-scattered images in the absence of neutron aperture and scintillator point spread functions. Figure 1 shows the light emission curves modeled from various measurements for a variety of scintillators. The BCF99-55, BC422, Xylene[16], and DPAC 30 models are derived by Munro from recent preliminary cyclotron measurements of neutron florescence by Hatarick[17] ;the Liquid A([18])curve by Morgan from an Am-Be gamma ray source; and the EJ399 model from measurements by Barrera and Moran[19]. BCF99-55 is the material chosen for the first implementation of the NIF imager[9] and the EJ399 in the CEA liquid scintillator[3]. Xylene, DPAC-30, and Liquid A have not yet been used in neutron imaging.

For this study the neutron output of one THD capsule producing 4.45e+14 neutrons was used. The neutron fraction between 13 and 20 MeV is 81.6%; the down-scattered fraction (dsf), i.e. escaping neutrons between 10 and 12 MeV / 13-20 MeV, is 2.56%. This particular capsule is a stringent test of scintillator decay, since a well tuned THD implosion (higher convergence) with a dsf of ~ 7% would have a relatively larger signal. The image simulated from this capsule contains light from both 10-12 MeV neutrons arriving during the time gate, and from delayed light produced by earlier, faster neutrons. Figure 2 shows the primary (13.5-20 MeV) source and Figure 3 the downscattered (10-12 MeV) source. Figures 4, 5, and 6 show the gated images using EJ399, BCF99-55, and Liquid A. The Liquid A gated image is nearly identical to the down-scattered image (fig. 3) while the EJ399 image is similar to the primary (fig. 2). The BCF99-55 image needs correction. As Barrera[18] found before, the delayed light image is well approximated by a fraction of the primary image. Experimentally we will measure both the primary and gated image, and correct the gated image by subtracting a fraction of the primary, to obtain our best estimate of the down-scattered image. Computationally that fraction of the primary image represents 98.8% of the variance between the gated image and the down-scattered image. Experimentally the correction fraction will be measured with the primary and gated images from a directly driven glass capsule with very little down-scattering.

Using our decay models we can compare the magnitude of the delayed image, hence the amount of correction needed, for the different scintillators. These fractions are: EJ399, 7.7%; BC422, 2.6%; BC99-55,1.5%;Xylene, 1.2%;DPAC-30, 0.25%; and Liquid A, 0.1%. The total light in this residual image, compared to that in the gated image is: 70% for EJ399; 46% for BC422; 30% for BC99-55; 30% for Xylene; 8% for DPAC-30, and 3.4% for Liquid A. If the late image were gated for 9.5 to 11 MeV instead of 10 to 12, the delayed image would have been a smaller fraction of both the gated image and the of primary (4.0% for EJ399; 1.4% for BC422; 0.5% for BC99-55; 0.6 % for Xylene, 0.1% for DPAC-30, and 0.6% for Liquid A). However the light from 9.5-11 MeV neutrons is only ~50% of that from the 10-12, leading us to prefer the 10-12 MeV band for the down-scattered measurement. Of the three scintillators that have been incorporated into neutron imagers (EJ399, BC422, and BCF99-55), BCF99-55 is the best for down-scattered imaging at the NIF distance of 28m.

IV. Measuring the NIF Decayed Image at Omega

The decayed signal from the as-built 16x16 cm BCF99-55 NIF scintillator was measured on the Omega laser from the neutrons emitted by 875 μm OD, 15 μm thick plastic capsules filled with 15 atm DT gas, producing yields of ~2.2 e+13 neutrons No pinhole assembly was in the line of sight, but a 5 cm thick tungsten block was placed near the scintillator surface, 13 m from the target. The PMT was gated on between 44 and 104ns after the neutrons were generated, the same times as the will be used at 28 m on NIF. The DT rho-r from similar capsules is ~ 5-10 mg/cm^2 and the CH ~ 60 mg/cm^2 ([20]). With these rho-r's the expectation of the down-scattered neutrons in the 60 ns gate is < 0.1% of the primary signal. At 13 m a continuum of T+T neutrons does arrive during the gate, unlike at NIF. Although the TT yield is not measured, we can expect it to be ~ 0.5% of the DT yield, with ~0.1% arriving during the gate. Using the BCF99-55 model and a 5.5 keV burn temperature, we calculate the delayed light to be 1.0% during the gate. Reduction of the Omega data showed that the time integrated light from contemporaneous radiation interacting in the scintillator and residual decayed light during the gate to be ~ 0.7 ±0.5% of that from the primary. Including background, the residual light component may be as low as 0.2%. This measured low value and the 1.4 % calculated for the NIF system on THD capsules confirm the NIF NIS's ability to measure down-scattered neutron images.

ACKNOWLEDGEMENTS

This work was supported by U.S. Department of Energy Office of Inertial Confinement at Los Alamos National Laboratory, Lawrence Livermore National Laboratory, and NTEC , Los Alamos.

CAPTIONS

Fig. 1 Light émission from models of EJ399, BC422, BCF99-55, Xylene, DPAC 30, and Liquid A scintillators. At 28 m the 10-12 MeV image will be recorded between 44 and 100 ns.

Fig. 2 Figure 2. Primary neutron source from 13-20 MeV. Frame is 120x120 µm. The hohlraum axis is vertical.

Fig. 3 Figure 3 Down-scattered 10-12 MeV neutron source.Frame is 120x120 µm. 10-12 MeV Image

Fig. 4 Gated image between 44 and 104 ns from the EJ399 scintillator.

Fig. 5 Gated image between 44 and 104 ns from the BCF99-55 scintillator.

Fig. 6 Gated image between 44 and 104 ns from the BCF99-55 scintillator.

REFERENCES

1 D. Ress, R. A. Lerche, R. J. Ellis, S. M. Lane, K. A. Nugent, Science, **241**, 956 (1988).

2. C. R. Christensen, D. C. Wilson, C. W. Barnes, G. P. Grim, G. L. Morgan, M. D. Wilke, F. J. Marshall, V. Yu. Glebov, and C. Stoeckl, Phys. Plasmas 11, 2271 (2004).

3. L. Disdier, A. Rouyer, I. Lantuejoul, O. Landoas, J. L. Bourgade, T. C. Sangster, V. Yu. Glebov, R. A. Lerche, Phys. Plasmas, 13, 056317-1 (2006).

4. G. H. Miller, E. I. Moses, and C. R. Wuest, Nucl. Fusion 44, S228 (2004).

5. T. R. Boehly, D. Brown, R. Craxton, R. Keck, J. Knauer, J. Kelly, T. Kessler, S. Kumpan, S. Loucks, S. Letzring, F. Marshall, R. McCrory, S. Morse, W. Seka, J. Soures, and C. Verdon, Opt. Commun. **133**, 495 (1977).

6. D. C. Wilson, W. C. Mead, L. Disdier, M. Houry, J-L. Bourgade, and T.J. Murphy, Nuc. Instru. Meth. A, **488**, 400(2002).

7 D. C. Wilson, C. R. Christensen, G. L. Morgan, M. D. Wilke, P. A. Bradley, P. L. Gobby , Rev. Sci. Instrum., 74, 1705 (2003).

8 M. Moran, et al., Rev. Sci. Instrum., **75**, 3592 (2004).

9. M. D. Wilke, S. H. Batha, P. A. Bradley, R. D. Day, D. D.Clark, V. E. Fatherly, J. P. Finch, R. A. Gallegos, F. P. Garcia, G. L. Morgan, J. A. Oertel, T. A. Ortiz, J. R. Payton, P. Pazuchanics, D. W. Schmidt, A. C. Valdez, C. H. Wilde, D. C. Wilson, Rev. Sci. Instrum., **79**, 10E529 (2008).

10 D. S. Clark, S.W.Haan, B. A. Hammel, J. D. Salmonson, D. A. Callahan, and R. P. J. Town, Phys. Plasmas, 17, 052703 (2010).

11 D. C. Wilson, P. A. Bradley, H. W. Herrmann, B. K. Spears, C. J. Cerjan, J. D. Salmonson, S. P. Hatchett II, V. Yu. Glebov, Rev. Sci. Instrum. 79, 10E502(6), (2008)

12. M. M. Marinak, R. E. Tipton, O. L. Landen, T. J. Murphy, P. Amendt, S. W. Haan, S. P. Hatchett, C. J. Keane, r. McEachern, R. Wallace, Phys. Plasmas **3**, 2070 (1996).

13._V. Fatherley, R. Day, F. Garcia, G. Grim, J. Oertel, C. Wilde, M. Wilke, HTPD 2010, Rev. Sci. Instrum. , submitted May 2010.

14. I. Tregillis et al. HTPD 2010. HTPD 2010, Rev. Sci. Instrum. , submitted May 2010.

15. E. N. Loomis, G. P. Grim, C. Wilde, D. C. Wilson, G. Morgan, M. Wilke, I. Tregillis, F. Merrill, D. Clark, J. Finch, D. Fittinghoff, and D. Bower, HTPD 2010, Rev. Sci. Instrum. , submitted May 2010.

16 R. Lauck, M. Brandis, B. Bromberger, V. Dangendorf, M. B. Goldber, I. Mor, K. Tittelmeier, D. Vartsky, IEEE Trans. Nuc. Sci. **56**, 989 (2009).

17 R. Hatarick, Private Communication, Scintillator Workshop, LLNL, April 2010.

18 P. B. Lyons, S. E. Caldwell, L. P. Hocker, D. G. Crandall, P. A. Zagarino, J. Cheng, G. Tirsell, C. R. Hurlbut ,IEEE Transactions on Nuclear Science, 24, 177 (1977).

19 C. Barrera, U. C. Berkeley PhD Thesis, UCRL-TR-234115 (2007).

20 C. K. Li, F. H. Segin, J. A. Frenje et al. , Phys. Rev. Lett. 89, 165002-1 (2002).

Figure 1. Light émission from models of EJ399, BC422, BCF99-55, Xylene, DPAC 30, and Liquid A scintillators. At 28 m the 10-12 MeV image will be recorded between 44 and 100 ns.

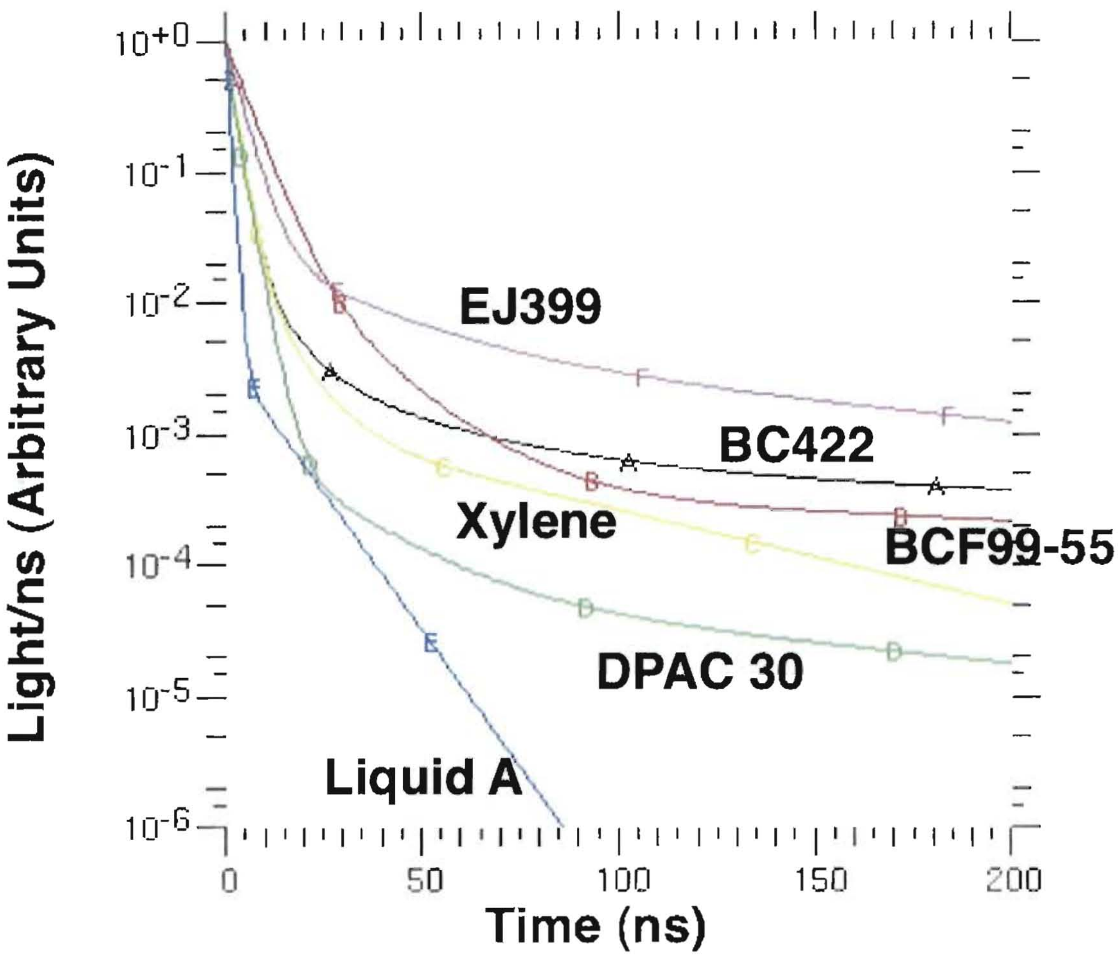

Figure 2. Primary neutron source from 13-20 MeV. Frame is 120x120 μm. The hohlraum axis is vertical.

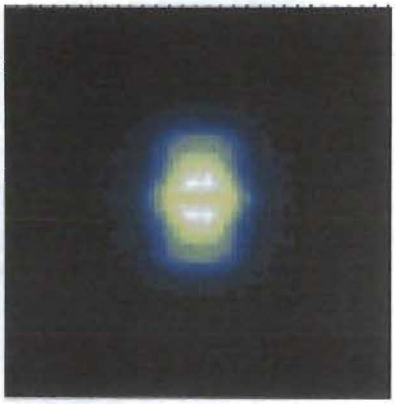

Figure 3 Down-scattered 10-12 MeV neutron source.Frame is 120x120 μm. 10-12 MeV

Image

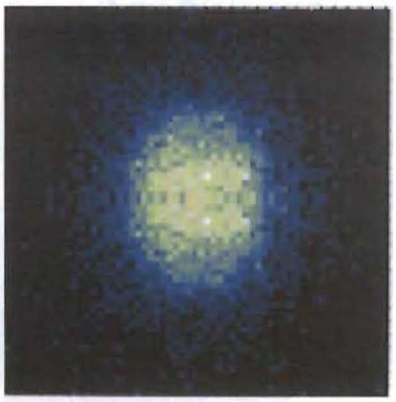

Figure 4. Gated image between 44 and 104 ns from the EJ399 scintillator.

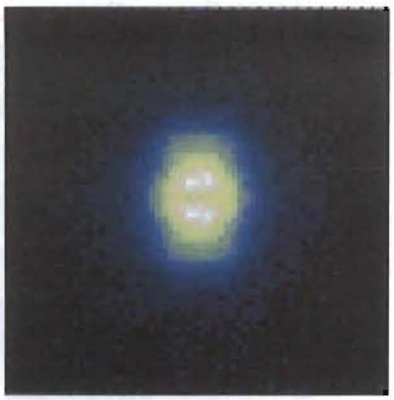

Figure 5 Gated image between 44 and 104 ns from the BCF99-55 scintillator.

Figure 6. Gated image between 44 and 104 ns from the Liquid A scintillator.